Atomic Level Structure in Multicomponent Bulk Metallic Glass

Y. Q. Cheng,[1] E. Ma,[1] and H. W. Sheng[2,*]

[1]Department of Materials Science and Engineering, Johns Hopkins University, Baltimore, Maryland 21218, USA
[2]Department of Computational and Data Sciences, George Mason University, Fairfax, Virginia 22030, USA

(Received 17 April 2008; published 17 June 2009)

The atomic-level structure of a representative ternary Cu-Zr-Al bulk metallic glass (BMG) has been resolved. Cu- (and Al-) centered icosahedral clusters are identified as the basic local structural motifs. Compared with the Cu-Zr base binary, a small percentage of Al in the ternary BMG leads to dramatically increased population of full icosahedra and their spatial connectivity. The stabilizing effect of Al is not merely topological, but also has its origin in the electronic interactions and bond shortening.

DOI: 10.1103/PhysRevLett.102.245501 PACS numbers: 61.43.Dq

For bulk metallic glasses (BMGs) that have emerged in recent years, a clear understanding of their internal structure is important for explaining their macroscopic properties [1]. Unfortunately, these complex amorphous structures pose at least three major challenges. (1) Recent studies have revealed that the ''solute centered quasiequivalent cluster'' can be viewed as the basic local structural motif in some solute-lean MGs [2–4]. But BMGs are mostly concentrated alloys that contain three or more elements [1]. (2) A direct experimental characterization (e.g., the total structure factor), combined with reverse Monte Carlo modeling, is usually insufficient to unambiguously reconstruct the 3D atomic packing of multicomponent BMGs. *Ab initio* simulations using the density functional theory would also encounter major difficulties, as discussed below. (3) The description of the atomic structure in a glass cannot be exact and is meaningful only in the statistical sense. The atomic-level structure of BMGs thus remains elusive and intriguing.

This work addresses three questions. First, can the structure of multicomponent BMGs be described in terms of cluster packing, characterized by the icosahedral order proposed previously for some simpler liquids and MGs [4–9]? Second, it is known that substituting a few percent of Al for Zr in the $Cu_{46}Zr_{54}$ alloy results in a remarkable decrease of the critical cooling rate needed for BMG formation [10], as well as pronounced differences in strength and ductility [11]. Is there, then, an obvious and quantifiable change of the BMG internal structure due to the alloying element? Third, is the alloying effect on structure purely topological, due to the known atomic size differences of the elements [2–4], or is it strongly influenced by the chemistry of the alloy, i.e., the intricate bonding environments? We stress that satisfactory answers to these questions do not exist at present, even though some simulations and fitting to x-ray data suggest icosahedral order [12–17].

We have chosen to study the $Cu_{46}Zr_{47}Al_7$ alloy, because the Cu-Zr-Al system is the basis of many important BMGs with interesting properties [11,18]. To unravel the atomic-level structure, we use a combination of *ab initio* molecular dynamics (MD) and embedded atom method (EAM) MD simulations. This is necessary because *ab initio* MD alone is often inadequate for solving the *structure* of multicomponent BMGs, although it provides high accuracy in calculating the energies and forces based on electronic structure. The reasons are: (1) The simulation time scale of *ab initio* MD is on the order of ~ps, and the resulting quenching rate ($\sim 10^{13}$ K/s) would be too rapid for the characteristic short-to-medium range order to develop in BMGs with multiple species and complex local environments [4]. (2) The system size is usually ~100 atoms, with only a few atoms for the alloying (solute) elements. Statistical fluctuation could thus be significant. Moreover, the periodic boundary conditions applied on the small box (~1 nm) may impose constraints on the type or degree of order developed. (3) Currently, *NPT* (constant number of particles, pressure and temperature) *ab initio* MD simulation is highly computationally intensive, which precludes simulation of the constant-pressure laboratory quenching experiments. The classical MD with the EAM potentials, on the other hand, can overcome these problems (time scale $>$ ns, system size $> 10,000$ atoms, and *NPT* ensemble), but it requires accurate and reliable EAM potentials. We report here (see Supplemental Material I [19]) our newly-developed EAM potentials for the Cu-Zr-Al ternary system, obtained by fitting the potential energy surface [20] surveyed via *ab initio* calculations (VASP [21]) of over 600 configurations, including crystalline phases, liquids and MGs, employing the force-matching approach (*potfit* [22]) and self-consistent recursive refinements. These potentials have been validated extensively, by comparing EAM-derived results with both *ab initio* and experimental data [19].

A 10 000-atom configuration of the $Cu_{46}Zr_{47}Al_7$ MG (inset in Fig. 1) was obtained using the EAM potentials we developed, via *NPT* quenching (zero pressure) from the melt (2000 K, equilibrium mass density 6.31 g/cc) to 300 K (6.95 g/cc) at 10^{10} K/s. The resulting partial pair distribution functions (PDFs) are shown in Fig. 1. The

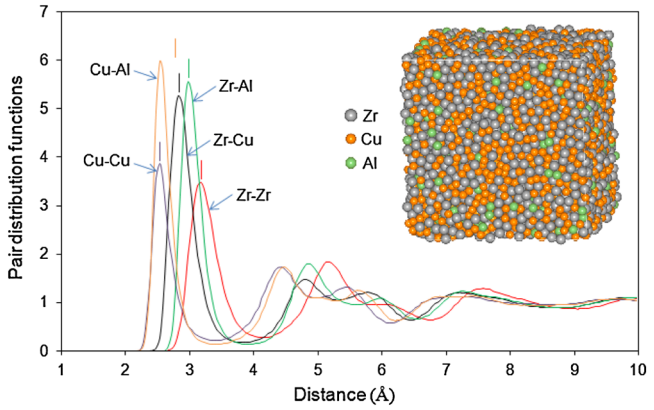

FIG. 1 (color online). Partial PDFs of an EAM MD-derived $Cu_{46}Zr_{47}Al_7$ MG configuration (inset). Vertical bars label the predicted bond length of each pair by adding the tabulated metallic radii. The obvious deviation observed for the Cu-Al pair indicates bond shortening. For clarity, the noisy and scattered Al-Al partial PDF is not included.

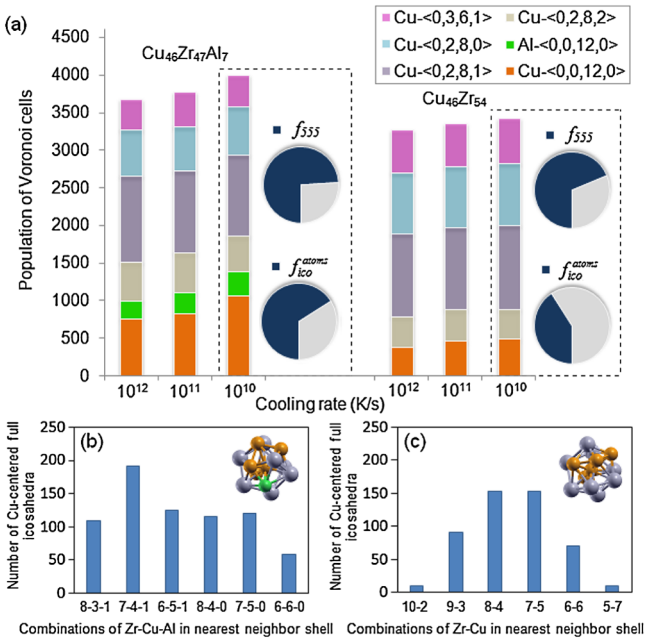

FIG. 2 (color online). (a) Histogram showing the polyhedra fractions with various Voronoi indices. Inset pie charts show $f_{\mathrm{ico}}^{\mathrm{atoms}}$ and f_{555}. Note that f_{ico} (and $f_{\mathrm{ico}}^{\mathrm{atoms}}$ and f_{555}) increases with decreasing MD cooling rate. (b) Zr-Cu(-Al) combinations in the shell of Cu-centered FI in $Cu_{46}Zr_{47}Al_7$, and (c) in $Cu_{46}Zr_{54}$. The insets in (b) and (c) show the representative FI (same color scheme as in Fig. 1 inset).

inherent structure of the 10 000-atom MG was then analyzed by sorting out the nearest-neighbor environment of each of the atoms of all the species present, in terms of Voronoi (coordination) polyhedra [4]. Our analysis reveals that the structure is best described by the Voronoi polyhedra centered around the smaller species (e.g., Cu). Figure 2(a) displays the populations of the five most populous types, accounting for ~80% of all the polyhedra around Cu (each of the other types is below 5% and not shown). It is clear from the Voronoi indices that most Cu atoms have a coordination number (CN) near 12, and their coordination polyhedra are dominated by fivefold symmetry and icosahedral types. For example, the full icosahedra (FI) with complete fivefold environment have Voronoi index $\langle 0, 0, 12, 0\rangle$, in which the center Cu bonds with 12 neighbors, and each and every of the 12 pairs has 5 common-neighbor atoms [9]. These pairs are referred to as "fivefold bonds." Figure 2(b) shows six dominant Zr-Cu-Al combinations that are observed to make up the first-neighbor shell of the Cu-centered FI. Note that these FI should not be considered as perfect in a geometric sense, as they consist of multiple species with different sizes and chemical properties. They are not even identical throughout the sample, but share one thing in common: the complete fivefold environment. We emphasize that the "full but not perfect/identical" feature is important, because the complete fivefold environment enhances the transition barrier to crystals [8], while the various bond lengths and angles and nonperfect shape reduce the chance to form quasicrystals or Frank-Kasper phases. The *amorphous* state is rendered more stable as a result. The FI found in the MG are also quite different from the local structures of possible competing crystals, e.g., $CuZr_2$ (with prototype $MoSi_2$ or $NiTi_2$ [19]).

Of all the Cu atoms in the MG configuration in Fig. 1, the fraction encaged in such FI, f_{ico}, is about 23%. But since each FI contains 13 atoms, the fraction of the total number of atoms involved in these FI, $f_{\mathrm{ico}}^{\mathrm{atoms}}$, is as high as ~66%. Meanwhile, several other types of polyhedra also contain many fivefold bonds, and are distorted or incomplete icosahedra. Of all the nearest-neighbor bonds around Cu, the fraction of fivefold bonds, f_{555}, is as high as 74% [Fig. 2(a)]. We thus conclude that interpenetrating Cu-centered icosahedra are the characteristic structural feature (additional Al-centered icosahedra are also included in Fig. 2(a), see discussion below).

The degree of icosahedral ordering found here exceeds by far those reported before in much worse glass formers such as $Ni_{60}Ag_{40}$ at a similar quench rate, for which f_{ico}, $f_{\mathrm{ico}}^{\mathrm{atoms}}$ and f_{555} are only 2%, 13%, and 25%, respectively [9]. A comparison is also made with the base binary $Cu_{46}Zr_{54}$ MG in Fig. 2(a). For $Cu_{46}Zr_{54}$ prepared under the same conditions (*NPT* quenching under zero pressure at 10^{10} K/s), f_{ico} drops to 11%, while the fractions of some distorted and incomplete icosahedra increase. The atoms involved, $f_{\mathrm{ico}}^{\mathrm{atoms}}$, decreases to ~41%. The bond angle distribution around Cu and bond orientation parameter Q_6 observed in a spherical harmonic analysis [6] exhibit the same trend (not shown). Evidently, alloying with 7% of Al greatly enhances the fivefold symmetry of the Cu-centered coordination polyhedra, making them more populous,

complete, and regular. This effectively lowers the energy and stabilizes the structure [23].

The FI overlap and connect by sharing vertex, edge, face, or tetrahedral bipyramid, as demonstrated in Figs. 3(a) and 3(b), which also illustrate the networks and/or superclusters formed as a result of the interconnection of the FI (leading to medium-range order). The spatial length scale (size), i.e., the degree of connectivity of FI that may serve as the backbone of the MG structure [24], is obviously higher in the ternary glass than in the binary [Figs. 3(c) and 3(d)].

Our results also indicate that more FI would get to form for slower cooling rates and this trend is more obvious for the ternary MG [Fig. 2(a)]. The BMGs formed in laboratory experiments at cooling rates orders of magnitude slower would hence contain even more FI than reported here. However, there is only minor difference between the simulated and experimental structure factors (Fig. S12 [19]). The reason is that the pair correlation is not sufficiently sensitive to the local adjustments of symmetry and regularity to reflect the effects of cooling rate on structure. As mentioned earlier, fitting only the two-body correlation is thus insufficient to reveal the structural details, substantiating the need for this MD study.

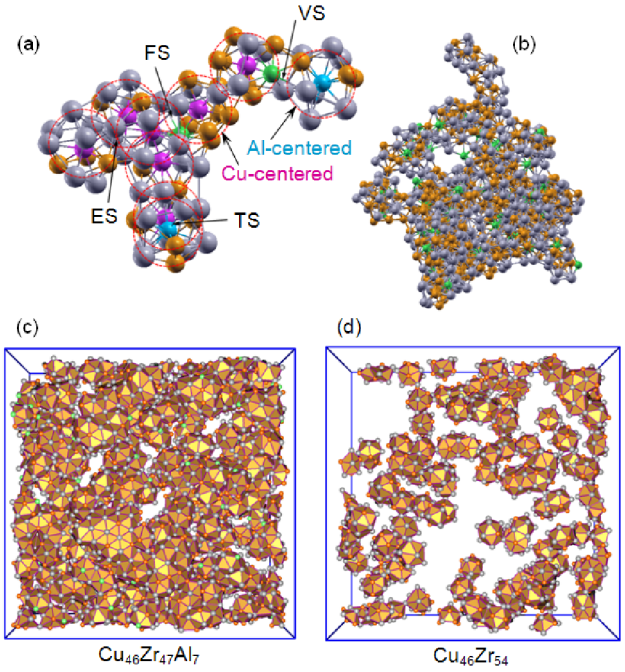

FIG. 3 (color online). (a) A supercluster consisting of 85 atoms, in 9 FI highlighted with dashed circles (the Cu *centers* are colored pink and Al *centers* blue, as labeled in the figure). VS (vertex sharing), ES (edge sharing), FS (face sharing), and TS (tetrahedra sharing, i.e., interpenetrating) represent typical sharing schemes. (b) A large supercluster consisting of 736 atoms (103 FI, ~2 nm in size) found in $Cu_{46}Zr_{47}Al_7$. The degree of connectivity of the FI is obviously higher in (c) for $Cu_{46}Zr_{47}Al_7$ than in (d) for $Cu_{46}Zr_{54}$. For clarity, only the top half of the simulation box is shown in (c) and (d).

We next address the key question as to why icosahedra develop so prominently in these BMGs, particularly in the ternary one. The ideal icosahedral dense packing requires an atomic size ratio R^* of 0.902 for a hard-sphere packing model [6], where $R^* = r_B/r_A$, and r_A and r_B are the atomic radii of the solvent atoms in the nearest-neighbor shell and the center solute, respectively. For binary Cu-Zr, $r_{Zr} = 1.58$ Å and $r_{Cu} = 1.27$ Å [18] and R^* is 0.804, such that icosahedral packing would not be topologically stable/efficient when Cu is completely surrounded by Zr. It would not be possible, however, to encage every Cu by Zr atoms only, when the Cu concentration is high ($Cu_{46}Zr_{54}$) and the heat of mixing (ΔH_{mix}) is highly negative. Instead, Zr atoms mix with Cu [e.g., 8 Zr with 4 Cu, inset of Fig. 2(c)] in the first-neighbor shell of Cu. This allows the leeway for adjusting the relative proportions of Zr and Cu, facilitating icosahedral packing.

Al further promotes icosahedral ordering in two ways. First, an Al atom can be found among the first-shell neighbors of the Cu, Fig. 2(b). Because Al has a radius in between those of Zr and Cu, we now have three atomic sizes to adjust the coordination polyhedron around the Cu. This increases the possibility of comfortable arrangements to reach the FI. As seen in Fig. 2(b), compared with $Cu_{46}Zr_{54}$ [Fig. 2(c)], $Cu_{46}Zr_{47}Al_7$ has more first-neighbor combinations that contribute rather evenly to the FI formation.

Second, the negative ΔH_{mix} of Al with Zr and Cu drives Al to scatter in the Cu-Zr matrix. For the Al-centered polyhedra, fivefold bonds are also dominant (~80%), and the $\langle 0, 0, 12, 0\rangle$ FI are the most popular (~46%). We note that the atomic size ratio, r_{Al}/r_{Zr}, is 0.905, which is rather close to the ideal ratio of 0.902. This would suggest that Al surrounded by Zr *only* would be the topologically optimal way for FI packing. However, formation of a considerable amount of such Al-Zr icosahedra requires local segregation in this MG, which is unlikely since the composition of this alloy is rather rich in Cu, and the calculated ΔH_{mix} is negative between any two species [19]. In fact, most Al-centered FI in our simulated $Cu_{46}Zr_{47}Al_7$ have mixed atomic species in the shell.

Then, why are these Al-centered FI with ''mixed'' shell still favored (stable and populous)? As shown in Fig. 1, the interatomic distance between Al and Cu is noticeably smaller (by about 6%) than the sum of their tabulated metallic radii. This shortened bond length is known to exist in some Al-Cu intermetallics [25] (also, in Al-Fe and some other Al-TM MGs [26]), due to the coupling between the broad conduction band of Al and the narrow low-lying *d* band of Cu [27]. *Ab initio* calculations reported in Supplemental Material II [27] suggests unusual charge density distribution between Al and Cu, and the projected electron density of state shows evidence of special *sp-d*

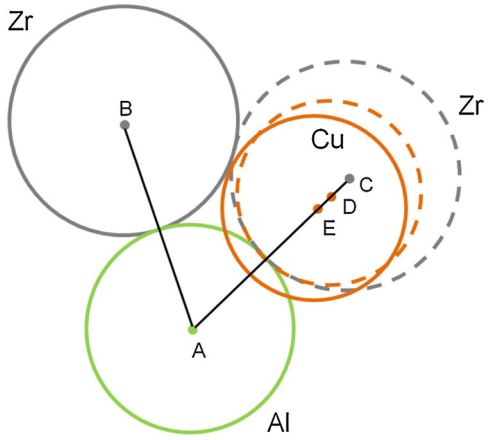

FIG. 4 (color online). A schematic (with scaled sizes and distances) showing how Al-Cu bond shortening facilitates the FI formation. Since r_{Al}/r_{Zr} is 0.905, Al can be surrounded by 12 Zr only to form a densely packed FI. Here, we display the Al (green circle A) and two neighboring Zr atoms (gray circles, solid B and dashed C). Now we substitute a Zr (C) with a Cu atom. In the absence of bond shortening, this Cu would take the position centered at D (the dashed orange circle), leaving an empty space between Zr and Cu in the shell. But since the Al-Cu bond is shortened, the actual center position of the Cu is at E, eliminating the empty space to allow full contact of Cu with Zr atoms.

interactions, which could be the electronic basis of the Al-Cu bond shortening. With the bond shortening, from the standpoint of the center Al, the Cu neighbor appears closer and "larger," in the sense that Cu effectively occupies the space around Al, in a way similar to Zr. This scenario is illustrated in Fig. 4. As a result, the special and shortened Al-Cu bond allows chemistry (stable bonding) and topology (dense packing) to work in concert, stabilizing and facilitating the formation of Al-centered FI in $Cu_{46}Zr_{47}Al_7$. In addition, for the Cu-centered icosahedra, the strong interaction of Al (in the shell) with both Zr and Cu also impart stabilizing effects.

Note that bond shortening and icosahedral order have also been identified as the major structural features in the *ab initio* MD-derived $Cu_{46}Zr_{47}Al_7$ MG (Fig. S10 [19]; a quantitative match between the fractions of each and every type of the polyhedra is not expected due to the reasons discussed earlier in this Letter).

In summary, we have developed EAM potentials for the Zr-Cu-Al system [19]. The structure of the typical Cu-Zr-Al BMG is best dissected from the vantage point of overlapping icosahedral motifs centered around Cu and Al, with different species mixed to several favorable ratios in the first shell. From the quantitative f_{ico}, f_{ico}^{atoms} and f_{555} results and their cooling rate dependence in Fig. 2(a), it can be inferred that icosahedral ordering (especially the FI with complete fivefold environment) should be the overwhelming structural feature in these BMGs obtained at laboratory cooling rates. The alloying of Al into Cu-Zr is particularly effective, as manifested not only by a large jump in the fraction of icosahedral clusters, but also by their improved symmetry (FI), as well as their enhanced spatial connectivity and medium-range order (Fig. 3). The local order does not come merely from straightforward topological packing of hard spheres of known (fixed) sizes, but is also affected by the chemistry of the specific alloy. As supported by *ab initio* calculations, electronic interactions involving Al are bond-specific and environment-specific [27]; the associated bond shortening can strongly influence the type, frequency, and stability of the coordination polyhedra.

This work was supported by US DOE, BES, Division of Materials Science and Engineering under Contract No. DE-FG02-09ER46056.

*hsheng@gmu.edu

[1] A. L. Greer and E. Ma, MRS Bull. **32**, 611 (2007).
[2] D. B. Miracle, Nature Mater. **3**, 697 (2004).
[3] D. B. Miracle, Acta Mater. **54**, 4317 (2006).
[4] H. W. Sheng *et al.*, Nature (London) **439**, 419 (2006).
[5] F. C. Frank, Proc. R. Soc. A **215**, 43 (1952).
[6] D. R. Nelson and F. Spaepen, Solid State Phys. **42**, 1 (1989).
[7] T. Schenk *et al.*, Phys. Rev. Lett. **89**, 075507 (2002).
[8] K. F. Kelton *et al.*, Phys. Rev. Lett. **90**, 195504 (2003).
[9] W. K. Luo *et al.*, Phys. Rev. Lett. **92**, 145502 (2004).
[10] P. Yu, H. Y. Bai, M. B. Tang, and W. L. Wang, J. Non-Cryst. Solids **351**, 1328 (2005).
[11] G. Kumar *et al.*, Scr. Mater. **57**, 173 (2007).
[12] K. Saksl *et al.*, Appl. Phys. Lett. **83**, 3924 (2003).
[13] S. Mechler *et al.*, Appl. Phys. Lett. **91**, 021907 (2007).
[14] P. Zetterström *et al.*, J. Phys. Condens. Matter **19**, 376217 (2007).
[15] N. Jakse and A. Pasturel, Appl. Phys. Lett. **93**, 113104 (2008).
[16] N. Fujima *et al.*, Mater. Trans., JIM **48**, 1734 (2007).
[17] X. D. Wang *et al.*, Appl. Phys. Lett. **92**, 011902 (2008).
[18] D. H. Xu, G. Duan, and W. L. Johnson, Phys. Rev. Lett. **92**, 245504 (2004).
[19] See EPAPS Document No. E-PRLTAO-103-011927 for supplemental materials. For more information on EPAPS, see http://www.aip.org/pubservs/epaps.html.
[20] F. H. Stillinger, Science **267**, 1935 (1995).
[21] G. Kresse and J. Furthmüller, Comput. Mater. Sci. **6**, 15 (1996); P. E. Blöchl, Phys. Rev. B **50**, 17953 (1994); G. Kresse and D. Joubert, Phys. Rev. B **59**, 1758 (1999).
[22] P. Brommer and F. Gähler, Model. Simul. Mater. Sci. Eng. **15**, 295 (2007).
[23] X. K. Xi *et al.*, Phys. Rev. Lett. **99**, 095501 (2007).
[24] Y. Shi and M. L. Falk, Scr. Mater. **54**, 381 (2006).
[25] M. Widom, I. Al-Lehyani, and J. A. Moriarty, Phys. Rev. B **62**, 3648 (2000).
[26] K. Ahn *et al.*, Phys. Rev. B **70**, 224103 (2004).
[27] See EPAPS Document No. E-PRLTAO-103-011927 for supplemental materials. For more information on EPAPS, see http://www.aip.org/pubservs/epaps.html.